19. M. J. Wade, *Nat. Rev. Genet.* **8**, 185–195 (2007).
20. R. Honegger, *New Phytol.* **103**, 785–795 (1986).
21. J. M. Gómez, M. Verdú, F. Perfectti, *Nature* **465**, 918–921 (2010).
22. W. Harcombe, *Evolution* **64**, 2166–2172 (2010).
23. K. L. Hillesland, D. A. Stahl, *Proc. Natl. Acad. Sci. U.S.A.* **107**, 2124–2129 (2010).
24. N. Klitgord, D. Segrè, *PLOS Comput. Biol.* **6**, e1001002 (2010).
25. B. Momeni, C. C. Chen, K. L. Hillesland, A. Waite, W. Shou, *Cell. Mol. Life Sci.* **68**, 1353–1368 (2011).

ACKNOWLEDGMENTS

We thank Q. Justman, B. Stern, A. Pringle, S. Sasso, M. Dayel, N. Collins, J. Hess, M. Mueller, G. Frenkel, S. Kryazhimskiy, M. McDonald, D. Van Dyken, E. Wallace, K. Zimmerman, P. Boynton, J. Calarco, D. Chiang, Y. Eun, K. Foster, R. Losick, W. Tong, Y. Katz, and members of the Murray and Nelson labs for helpful feedback. We thank D. Thompson, M. Dunham, F. Winston, and N. Rhind for yeast strains; T. Schinko and J. Strauss for *A. nidulans* strains; and the Fungal Genetics Stock Center (Kansas City, MO) for fungal strains. We thank P. Rogers, M. Tam, and B. Tilton (Faculty of Arts and Sciences Center for Systems Biology FACS Core); B. Goetze, C. Kraft, and D. Richardson (Harvard Center for Biological Imaging); M. Yankova and S. King (Central Electron Microscopy Facility, University of Connecticut Health Center) for their resources and assistance; and U. Goodenough for her help in interpreting electron micrographs. Supported in part by a Jane Coffin Childs postdoctoral fellowship to E.F.Y.H. and by the National Institute of General Medical Sciences Center for Modular Biology (NIH grant P50-GM068763). Additional data described in this work can be found in the online supplementary materials. E.F.Y.H. conceived the project, performed the experiments, and analyzed the data. E.F.Y.H. and A.W.M. devised the research and wrote the manuscript. A.W.M. supported and provided input throughout all stages of this work.

SUPPLEMENTARY MATERIALS

www.sciencemag.org/content/345/6192/94/suppl/DC1
Materials and Methods
Figs. S1 to S7
Tables S1 to S8
Movies S1 to S16
References (*26*–*71*)

13 March 2014; accepted 22 May 2014
10.1126/science.1253320

CELL DEATH

Opposing unfolded-protein-response signals converge on death receptor 5 to control apoptosis

Min Lu,[1*] David A. Lawrence,[1*] Scot Marsters,[1] Diego Acosta-Alvear,[2,3] Philipp Kimmig,[2,3] Aaron S. Mendez,[2,3] Adrienne W. Paton,[4] James C. Paton,[4] Peter Walter,[2,3]† Avi Ashkenazi[1]†

Protein folding by the endoplasmic reticulum (ER) is physiologically critical; its disruption causes ER stress and augments disease. ER stress activates the unfolded protein response (UPR) to restore homeostasis. If stress persists, the UPR induces apoptotic cell death, but the mechanisms remain elusive. Here, we report that unmitigated ER stress promoted apoptosis through cell-autonomous, UPR-controlled activation of death receptor 5 (DR5). ER stressors induced *DR5* transcription via the UPR mediator CHOP; however, the UPR sensor IRE1α transiently catalyzed *DR5* mRNA decay, which allowed time for adaptation. Persistent ER stress built up intracellular DR5 protein, driving ligand-independent DR5 activation and apoptosis engagement via caspase-8. Thus, DR5 integrates opposing UPR signals to couple ER stress and apoptotic cell fate.

The endoplasmic reticulum (ER) mediates folding and maturation of transmembrane and secreted proteins (*1*, *2*). Elevated physiological demand for protein folding can cause misfolded proteins to accumulate in the ER lumen—a condition called ER stress. The unfolded protein response (UPR) senses such stress and mediates cellular adaptation by expanding the ER's protein-folding capacity while decreasing its synthetic load. Protein kinase R (PKR)–like kinase (PERK) and inositol-requiring enzyme 1α (IRE1α) are two key metazoan UPR sensors (*1*, *2*); residing in the ER membrane, each has a lumenal domain that detects misfolded polypeptides. PERK harbors a cytoplasmic kinase moiety that phosphorylates eukaryotic translation-initiation factor 2α (eIF2α). This suppresses general translation but promotes synthesis of preferred factors—including ATF4, which activates the UPR transcription factor CCAAT/enhancer-binding protein homologous protein (CHOP), among other genes. IRE1α has both kinase and endoribonuclease (RNase) cytoplasmic moieties (*3*). The kinase controls RNase activity, which mediates regulated IRE1α-dependent decay (RIDD) of ER-associated mRNAs (*4*) and generates the UPR transcription factor X-box binding protein 1 spliced (XBP1s). Certain pathological conditions can cause irresolvable ER stress (*5*), often leading to apoptotic cell death (*1*, *2*, *6*). Two interconnected signaling cascades control apoptosis: the intrinsic, mitochondrial pathway, and the extrinsic, death-receptor pathway (*7*). Each engages distinct proteases, called initiator caspases, to activate a common set of executioner caspases (*8*). Unmitigated ER stress regulates the intrinsic pathway via several Bcl-2 family proteins (*1*, *2*, *6*, *9*, *10*). Furthermore, IRE1α cleaves specific micro-RNAs to derepress caspase-2 expression (*11*); however, caspase-2 may be dispensable for ER stress-induced apoptosis (*12*), which leaves the underlying initiation mechanisms obscure.

[1]Cancer Immunology, Genentech, Inc., 1 DNA Way, South San Francisco, CA 94080, USA. [2]Howard Hughes Medical Institute, University of California, San Francisco, CA 94158, USA. [3]Department of Biochemistry and Biophysics, University of California, San Francisco, CA 94158, USA. [4]Research Centre for Infectious Diseases, School of Molecular and Biomedical Science, University of Adelaide, South Australia, 5005, Australia.
*These authors contributed equally to this work. †**Corresponding author. E-mail: peter@walterlab.ucsf.edu (P.W.); aa@gene.com (A.A.)**

Experiments with biological and pharmacological ER stressors revealed consistent activation of caspase-8, the pivotal initiator in the extrinsic pathway (*8*) (Fig. 1). The bacterial AB5 subtilase cytotoxin SubAB induces pathophysiological ER stress by cleaving the chaperone BiP (*13*). SubAB caused dose-dependent BiP depletion and ER stress, evident by CHOP and XBP1s up-regulation, in KMS11 multiple myeloma cells (Fig. 1A). In keeping with data that PERK activity persists, whereas IRE1α activation is transient (*14*), CHOP remained elevated, whereas XBP1s declined by 24 hours. SubAB also induced activation of caspase-8 and caspase-3 by 24 hours, evident by cleaved caspase and poly(ADP ribose) polymerase (PARP) products. SubAB substantially increased caspase-8 and caspase-3/7 enzymatic activity, and DNA fragmentation—an apoptotic hallmark (fig. S1, A to C). Brefeldin-A (BfA)—an inhibitor of ER-to-Golgi trafficking—similarly induced ER stress, caspase activation, and apoptosis in SK-MES-1 lung carcinoma cells (Fig. 1B and fig. S1, D to F). The sarcoplasmic ER calcium–adenosine triphosphatase inhibitor thapsigargin (Tg) induced persistent CHOP and transient XBP1s expression in wild-type and in *Bax*$^{-/-}$ HCT116 colon carcinoma cells; whereas apoptosis required *Bax*, caspase-8 activation did not (Fig. 1, C and D, and fig. S1, G to I). Moreover, small interfering RNA (siRNA) depletion of caspase-8, but not caspase-2, blocked activation of caspase-3/7 and apoptosis by diverse ER stressors (Fig. 1, E and F, and fig. S1, J to O). Caspase-8 activates the Bcl-2 family protein Bid to engage the intrinsic pathway via Bax (*15*, *16*). Full-length Bid declined in association with Tg-induced caspase-8 activation (fig. S1I), which indicated Bid processing. Bid siRNA knockdown commensurately attenuated Tg-induced apoptosis, whereas caspase-8 siRNA inhibited both Bid processing and apoptosis (fig. S1, P to S). Tg also up-regulated Bim (fig. S1I) as reported (*10*); however, caspase-8 and Bid processing occurred much earlier, which suggests that Bim might support later apoptotic signals. Thus, caspase-8 plays a pivotal role, whereas caspase-2 appears dispensable, during apoptosis induction by unmitigated ER stress.

Upon binding of cognate extracellular ligands, the death receptors Fas, DR4, or DR5 nucleate a death-inducing signaling complex (DISC) at the plasma membrane, which activates caspase-8 via

the adaptor Fas-associated death domain (FADD) (*17*). Consistent with evidence that ER stress up-regulates *DR5* transcription (*18*), quantitative reverse transcription polymerase chain reaction (QPCR) showed a two- to fourfold *DR5* mRNA induction by Tg, BfA, SubAB, or the glycosylation inhibitor tunicamycin (Tm), with less impact on *DR4*, *Fas*, or *TNFR1* (Fig. 2, A and B, and fig. S2, A to C). ER stressors most often elevated both the long (DR5L) and short (DR5S) splice variants of DR5 (Fig. 2C and fig. S2, D to H) (*19*). Tg up-regulated DR5 within 6 hours, in concert with CHOP and XBP1s induction, yet preceding caspase-8 processing (Fig. 2C and fig. S2D). Furthermore, Tg induced a DR5-nucleated complex with FADD and caspase-8, harboring elevated caspase-8 activity, independent of *Bax* (Fig. 2D and fig. S2, I to K). Immunoprecipitation (IP) of DR5 or caspase-8 showed comparable caspase-8 activity (fig. S2L). Consistently, other ER stressors increased DR5-associated caspase-8 activity in multiple cell lines (fig. S2, M to O). Livers from Tm-treated mice also showed elevated DR5 and cleaved caspase-8 in conjunction with apoptosis (fig. S2, P and Q). DR5 siRNA knockdown in different cell lines strongly inhibited caspase activation and apoptosis in response to various ER stressors (Fig. 2, E to H, and fig. S2, R to X). Thus, DR5 is critical for caspase-8–mediated apoptotic engagement by unmitigated ER stress.

Remarkably, siRNA depletion of the sole DR5 ligand, Apo2L/TRAIL (apo2 ligand/tumor necrosis factor–related apoptosis-inducing ligand), had no impact on Tg-induced apoptosis in HCT116 or SK-MES-1 cells, unlike caspase-8 knockdown (Fig. 3A and fig. S3, A and B). Moreover, neutralization of extracellular Apo2L/TRAIL by using soluble DR4- and DR5-Fc fusion proteins, which blocked exogenously added ligand, did not inhibit apoptosis activation by Tg or BfA (Fig. 3B and fig. S3, C and D). Thus, ER stress induces ligand-independent DR5 activation. DR5 was barely detectable by immunofluorescence in resting SK-MES-1 cells but showed higher abundance with the addition of Tg or BfA (Fig. 3C). In Tg-treated cells, DR5 colocalized with the Golgi marker RACS1 but not the ER marker KDEL; however, in BfA-treated cells—which had minimal Golgi—DR5 did colocalize with KDEL (Fig. 3D and fig. S3, E and F). Despite massively elevating total DR5, BfA did not substantially up-regulate cell surface DR5, nor did it increase sensitivity to exogenous Apo2L/TRAIL (fig. S3, G to J). However, Tg, which up-regulated both total and cell surface DR5, did enhance sensitivity to added ligand (fig. S3, K to N). DR5 partially colocalized with cleaved caspase-8 within Tg-treated cells (fig. S3O), which supports intracellular activation. Size-exclusion chromatography of detergent extracts from HCT116 cells revealed Tg-driven up-regulation of DR5L and DR5S in low molecular weight (MW) fractions—representing DR5 oligomers; elevated DR5L appeared also in high

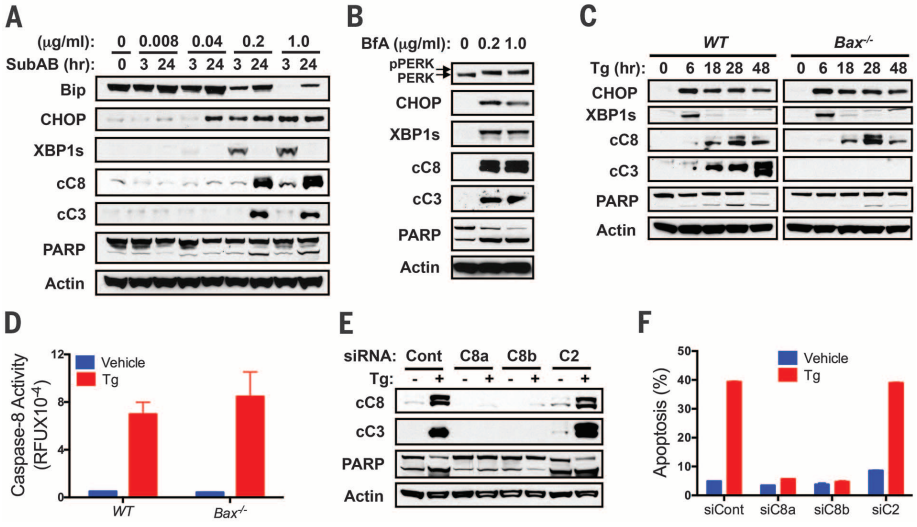

Fig. 1. Unmitigated ER stress triggers apoptosis via caspase-8. (**A**) KMS11 cells were treated with SubAB and analyzed by immunoblot. cC8: cleaved caspase-8; cC3: cleaved caspase-3. (**B**) SK-MES-1 cells were treated with BfA (24 hours) and analyzed by immunoblot. (**C** and **D**) Wild-type (WT) or *Bax*$^{-/-}$ HCT116 cells were treated with Tg (100 nM) and analyzed by immunoblot (C), or caspase-8 activity assay (24 hours) (D). (**E** and **F**) HCT116 cells were transfected (48 hours) with control siRNA (Cont), a single (C8a), or an independent pool (C8b) of caspase-8 siRNAs, or caspase-2 siRNA. Cells were treated with Tg (100 nM, 24 hours) and analyzed by immunoblot (E) or FACS to measure apoptosis by subG$_1$ DNA content (F). Graphs depict means ± SD of triplicates (D) or duplicates (F).

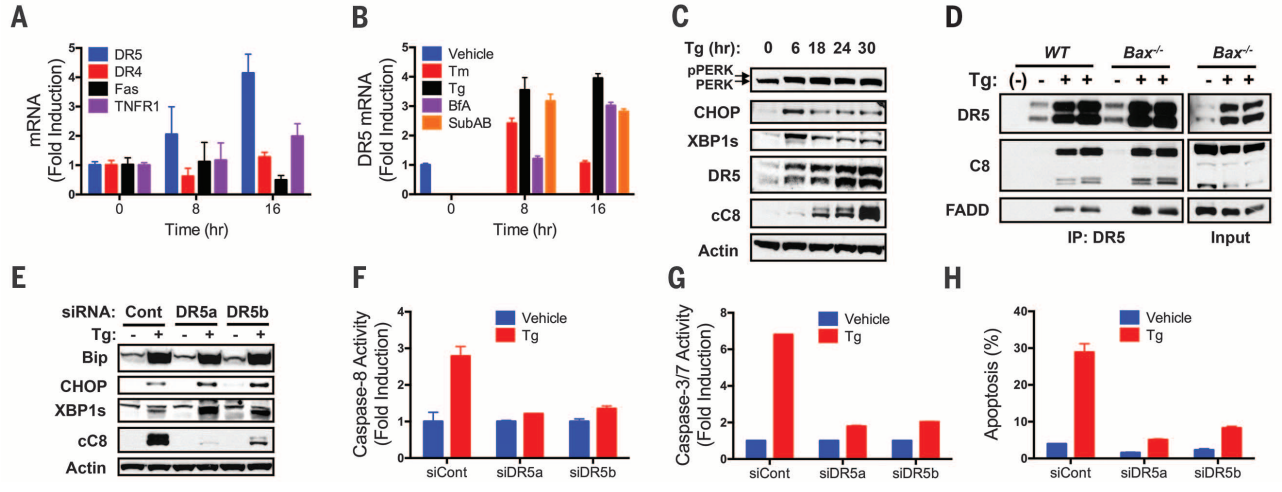

Fig. 2. Unmitigated ER stress activates caspase-8 via DR5. (**A**) HCT116 cells were treated with Tg (100 nM), and mRNA levels were measured by QPCR [normalized to glyceraldehyde-3-phosphate dehydrogenase (GAPDH)]. (**B**) HCT116 cells were treated with Tm (1 μg/ml), Tg (100 nM), BfA (1 μg/ml), or SubAB (1 μg/ml) and analyzed by QPCR (normalized to GAPDH). (**C**) HCT116 cells were treated with Tg (100 nM) and analyzed by immunoblot. (**D**) WT or *Bax*$^{-/-}$ HCT116 cells were treated as in (C) (24 hours), subjected to DR5 IP, and analyzed by immunoblot. (**E** to **H**) HCT116 cells were transfected (48 hours) with control siRNA (Cont), a single (DR5a), or an independent pool (DR5b) of DR5 siRNAs; then treated with Tg (100 nM, 24 hours) and analyzed by immunoblot (E), by enzymatic activity assay for caspase-8 (F) or caspase-3/7 (G), or by FACS for apoptosis (H). Graphs depict means ± SD of triplicates.

MW fractions—which indicates the presence of DR5L multimers (Fig. 3E). Caspase-8 activity occurred in two peaks: one coinciding with DR5L in high MW fractions, the other separate from DR5 in low MW compartments (Fig. 3F). Chemical cross-linking verified Tg-induced formation of DR5 oligomers and multimers (fig. S3P). Furthermore, selective DR5L siRNA knockdown attenuated Tg-driven activation of caspase-8 and apoptosis (fig. S3, Q to T). Thus, Tg up-regulates both DR5 variants but DR5L preferentially multimerizes, recruiting and activating caspase-8 and releasing processed enzyme into lower MW fractions.

Consistent with earlier evidence (*18*, *20*), siRNA depletion of CHOP substantially blocked *DR5* mRNA up-regulation by Tg or BfA, whereas knockdown of the CHOP transcriptional targets ER oxidase 1α (ERO1α) or growth arrest and DNA damage–inducible 34 (GADD34) did not (Fig. 4A and fig. S4, A to E); these findings support direct CHOP control of *DR5* mRNA. Although GADD34 dephosphorylates eIF2α to reinitiate translation, ERO1α is important for protein disulfide isomerization and folding in the ER lumen (*6*). ERO1α knockdown did inhibit DR5L protein up-regulation and the associated apoptotic events (fig. S4, F to H), which suggests that ERO1α may facilitate folding of DR5L (DR5L harbors more cysteine residues than DR5S). In contrast to CHOP depletion, siRNA knockdown of IRE1α attenuated *DR5* mRNA decay in Tg-treated cells (Fig. 4B and fig. S4, I to L), which suggests that IRE1α counter-

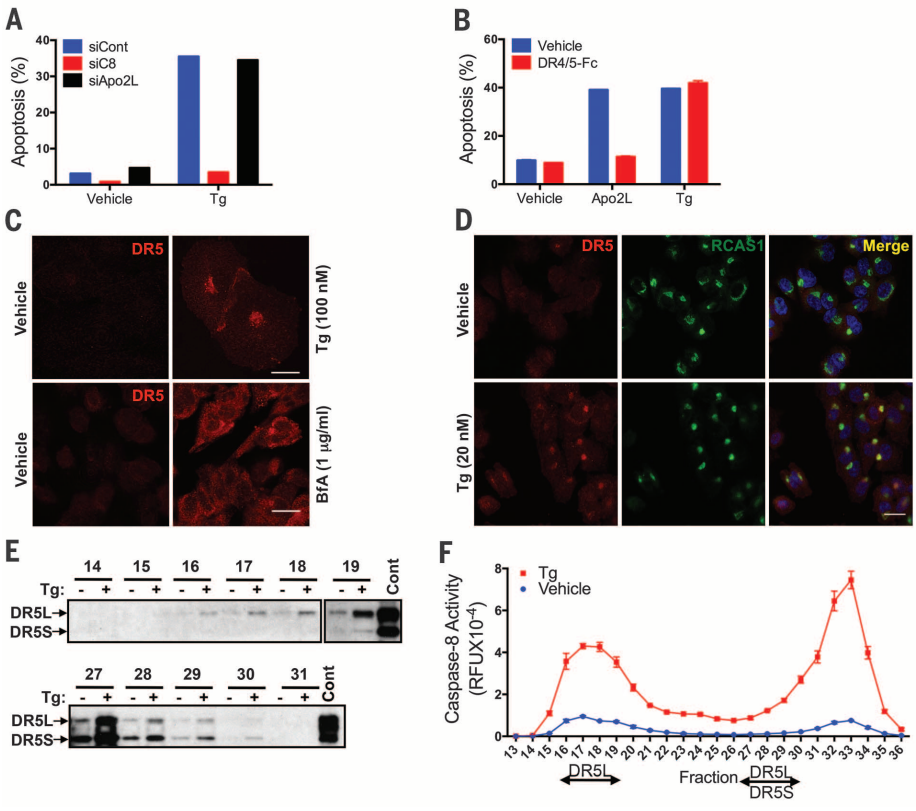

Fig. 3. Unmitigated ER stress engages caspase-8 by inducing ligand-independent intracellular DR5 activation. (**A**) HCT116 cells were transfected (48 hours) with control siRNA or siRNA targeting Apo2L/TRAIL or caspase-8. Cells were treated with Tg (100 nM, 24 hours) and analyzed for apoptosis. (**B**) HCT116 cells were treated (24 hours) with Apo2L/TRAIL (1 μg/ml) or Tg (100 nM) in the presence of vehicle or DR4-Fc plus DR5-Fc (10 μg/ml each) and analyzed for apoptosis. (**C**) SK-MES-1 cells were treated (16 hours) with indicated ER stressors and analyzed by immunofluorescence with DR5-specific antibody. (**D**) SK-MES-1 cells were treated with Tg (20 nM, 24 hours) and analyzed by immunofluorescence for DR5 or RACS1. (**E** and **F**) HCT116 cells were treated with Tg (100 nM, 24 hours), extracted with 1% Triton X-100, and subjected to size-exclusion chromatography; fractions were analyzed by DR5 IP and immunoblot (E) or caspase-8 activity assay (F). Control: direct DR5 IP from Tg-treated cells. Graphs depict means ± SD of duplicates (B) or triplicates (F). Scale bars: 20 μm (C and D).

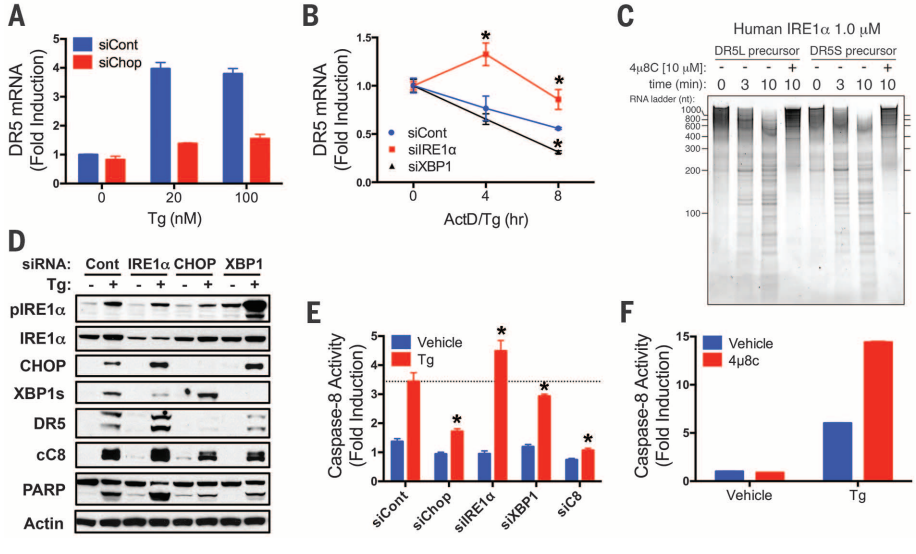

Fig. 4. DR5 integrates opposing UPR signals to control apoptosis. (**A**) HCT116 cells were transfected (48 hours) with control or CHOP siRNA, treated with Tg (8 hours), and analyzed by QPCR (normalized to GAPDH). (**B**) HCT116 cells were transfected (48 hours) with control, IRE1α, or XBP1 siRNA; and treated with actinomycin D (2 μg/ml) plus Tg (20 nM), then *DR5* mRNA was measured as in (A). (**C**) Purified recombinant human IRE1α comprising the kinase and RNase domains (KR43) was incubated with in vitro transcribed *DR5L* or *DR5S* mRNA in the presence of vehicle or 4μ8C (10 μM). Reactions were resolved on a 6% *Tris-borate-EDTA* (TBE)-urea polyacrylamide electrophoresis gel and stained with SYBR Gold. (**D** and **E**) HCT116 cells were transfected (48 hours) with control, IRE1α, CHOP, or XBP1 siRNA; treated with Tg (100 nM, 24 hours); and analyzed by immunoblot (D) or caspase-8 activity assay (E). (**F**) HCT116 cells were treated with Tg (100 nM, 24 hours) in the presence of vehicle or 4μ8C (30 μM) and analyzed for caspase-8 activity. Graphs depict means ± SD of triplicates.

acts apoptosis by mediating *DR5* RIDD. Indeed, a recombinant protein comprising IRE1α's catalytic domains cleaved in vitro transcribed *DR5* mRNAs at discrete sites, and this was blocked by the IRE1α RNase inhibitor 4μ8C (*21*) (Fig. 4C and fig. S4M). Furthermore, whereas CHOP siRNA attenuated Tg-induced DR5 up-regulation, caspase-8 activation, and apoptosis, IRE1α depletion augmented these events (Fig. 4, D and E, and fig. S4N). Conversely, XBP1s knockdown—which led to compensatory IRE1α hyperphosphorylation (Fig. 4D) as reported (*22*)—accelerated *DR5* mRNA decay and diminished DR5 up-regulation, caspase-8 activation, and apoptosis (Fig. 4, B, D, and E, and fig. S4, J to L and N). Finally, 4μ8C enhanced caspase activation by Tg (Fig. 4F and fig. S4O), which confirms an antiapoptotic role for IRE1α RNase. Thus, CHOP and RIDD exert opposing effects on *DR5* to control caspase-8 activation and apoptosis.

Our data delineate a cell-autonomous mechanism wherein DR5 integrates dynamic UPR signals to control apoptosis in relation to ER stress (fig. S4P). Upon reversible ER disruption, PERK-CHOP activity induces, whereas RIDD suppresses, *DR5* transcripts. If ER stress resolves, UPR activity subsides, and *DR5* mRNA returns to baseline. However, if ER stress prevails, PERK-CHOP function persists, whereas IRE1α activity attenuates (*14*), which permits *DR5* mRNA to rise. DR5 accumulation in the ER and Golgi apparatus drives ligand-independent multimerization of DR5L, which—consistent with earlier data (*23*)—has greater propensity to cluster than DR5S. ERO1α, previously implicated in UPR-driven apoptosis (*6*), facilitates DR5L up-regulation, perhaps by supporting disulfide isomerization. DR5L provides a DISC-like intracellular platform for caspase-8 recruitment and apoptosis initiation. It was proposed that ER stress augments apoptosis by increasing autocrine death-ligand signaling (*18*, *24*, *25*); however, ER disruption would attenuate ligand secretion. Our data reveal that *DR5* acts as an intracellular "gauge" for persistence of ER stress. Opposing controls on *DR5* mRNA synthesis and decay by PERK-CHOP versus IRE1α define a time window for adaptation, before committing the cell to an apoptotic fate.

REFERENCES AND NOTES

1. P. Walter, D. Ron, *Science* **334**, 1081–1086 (2011).
2. C. Hetz, *Nat. Rev. Mol. Cell Biol.* **13**, 89–102 (2012).
3. A. Korennykh, P. Walter, *Annu. Rev. Cell Dev. Biol.* **28**, 251–277 (2012).
4. J. Hollien, J. S. Weissman, *Science* **313**, 104–107 (2006).
5. S. Wang, R. J. Kaufman, *J. Cell Biol.* **197**, 857–867 (2012).
6. I. Tabas, D. Ron, *Nat. Cell Biol.* **13**, 184–190 (2011).
7. N. N. Danial, S. J. Korsmeyer, *Cell* **116**, 205–219 (2004).
8. G. S. Salvesen, A. Ashkenazi, *Cell* **147**, 476, e1 (2011).
9. H. Zinszner *et al.*, *Genes Dev.* **12**, 982–995 (1998).
10. H. Puthalakath *et al.*, *Cell* **129**, 1337–1349 (2007).
11. J.-P. Upton *et al.*, *Science* **338**, 818–822 (2012).
12. J. J. Sandow *et al.*, *Cell Death Differ.* **21**, 475–480 (2014).
13. A. W. Paton *et al.*, *Nature* **443**, 548–552 (2006).
14. J. H. Lin *et al.*, *Science* **318**, 944–949 (2007).
15. H. Li, H. Zhu, C. J. Xu, J. Yuan, *Cell* **94**, 491–501 (1998).
16. H. LeBlanc *et al.*, *Nat. Med.* **8**, 274–281 (2002).
17. N. S. Wilson, V. Dixit, A. Ashkenazi, *Nat. Immunol.* **10**, 348–355 (2009).
18. H. Yamaguchi, H. G. Wang, *J. Biol. Chem.* **279**, 45495–45502 (2004).
19. J. P. Sheridan *et al.*, *Science* **277**, 818–821 (1997).
20. M. Abdelrahim, K. Newman, K. Vanderlaag, I. Samudio, S. Safe, *Carcinogenesis* **27**, 717–728 (2006).
21. B. C. S. Cross *et al.*, *Proc. Natl. Acad. Sci. U.S.A.* **109**, E869–E878 (2012).
22. L. Niederreiter *et al.*, *J. Exp. Med.* **210**, 2041–2056 (2013).
23. K. W. Wagner *et al.*, *Nat. Med.* **13**, 1070–1077 (2007).
24. R. Martín-Pérez, M. Niwa, A. López-Rivas, *Apoptosis* **17**, 349–363 (2012).
25. P. Hu, Z. Han, A. D. Couvillon, R. J. Kaufman, J. H. Exton, *Mol. Cell. Biol.* **26**, 3071–3084 (2006).

ACKNOWLEDGMENTS

We thank R. Pitti and Genentech's peptide, DNA and chemical synthesis, and fluorescence-activated cell sorting (FACS) laboratories for assistance.

SUPPLEMENTARY MATERIALS

www.sciencemag.org/content/345/6192/98/suppl/DC1
Materials and Methods
Figs. S1 to S4
References (*26*–*30*)

3 April 2014; accepted 4 June 2014
10.1126/science.1254312

Supplementary Materials

Materials and Methods

Cell culture and experimental reagents

HCT116, SK-MES-1, KSM11, and RPMI-8226 cells were cultured in RPMI medium. Culture media were supplemented with 10% fetal bovine serum (FBS) and 2 mM L-glutamine. HCT116 $Bax^{-/-}$ cells were a kind gift from Dr Bert Vogelstein (*26*), Johns Hopkins University Medical School. Recombinant human DR4-Fc, DR5-Fc, TNFR1-Fc, and mouse anti-DR5 Abs were generated at Genentech (*27*), Inc. Tm, Tg, BfA, ActD were from Sigma. zVAD was from R&D systems. SubAB was prepared at the University of Adelaide, Australia, as described previously (*13*). IRE1α RNase inhibitor 4μ8c was synthesized at Genentech as described previously (*21*).

Antibody (Ab) for IP (mAb 5C7) or immunoblot (mAb 3H1) analysis of DR5 was generated at Genentech. For Immunofluorescence, either mouse anti-DR5 mAb 3H3 (Genentech) or rabbit anti-DR5 (Cell Signaling) was used. Abs for caspase-8 and KDEL were from Enzo Life Sciences. Ab for FADD was from BD BioScience. Ab for XBP1s was from BioLegend. Ab for caspase-2 was from Millipore. Cleaved caspase-8, cleaved caspase-3, PARP, Bip, PERK, Chop, Bid, Bim, ERO1α, IRE1α, RCAS1, Actin, and GAPDH Abs were from Cell Signaling Technology. Secondary antibodies were from GE Healthcare.

Mice

All mouse procedures were approved by and conformed to the guidelines and principles set by the Institutional Animal Care and Use Committee of Genentech and were carried out in an Association for the Assessment and Accreditation of Laboratory Animal Care (AAALAC)-accredited facility. C57BL/6 Mice were injected i.p. with Tm (1 mg/kg) or carrier (150 mM dextrose). Livers were collected and analyzed by immunoprecipitation with a mouse DR5 antibody (R&D Systems) followed by immunoblot with another mouse DR5 antibody (eBioscience). Alternatively, liver sections were subjected to TUNEL staining (Invitrogen) and imaged with a Leica SP5 inverted confocal microscope.

Caspase Activity and Apoptosis Assay

Caspase-8 or caspase-3/7 activity was measured using the Caspase-Glo 8 or Caspase-Glo 3/7 assay kits (Promega) that employ a luminogenic caspase-8 (IETD) or caspase-3/7 (DEVD) substrate. Measurements were done using a luminescence reader (Envision, Perkin Elmer), according to Promega's instructions. Caspase-8 activity in the DISC was measured by immunoprecipitating DISC components from cells using DR5 or caspase-8 pull down, followed by a Caspase-Glo 8 assay (Promega). Apoptosis was measured by sub-diploid DNA content: cells were fixed in 70% ethanol, stained with 50 μg/ml propidium iodide, treated with RNase A for 2 hr at 37°C, and analyzed by flow cytometry.

Transfection with siRNA Oligonucleotides

The siRNA oligonucleotides against human caspase-8, caspase-2, DR5, Bid, Apo2L/TRAIL, CHOP, IRE1α, XBP1, ERO1α, GADD34, and non-targeting controls were from Dharmacon. siRNAs against DR5L were designed as follows:
siDR5L(1) sense sequence: GCUGUGGAGGAGACGGUGAUU
siDR5L(2) sense sequence: CCUGUUCUCUCUCAGGCAUUU

Cells were transfected using Lipofectamine RNAiMAX (Invitrogen) according to the manufacturer's protocol.

Immunoprecipitation (IP) and Immunoblot Analysis

Cells were grown in 100 mm plates, treated as indicated, washed twice with cold PBS, and harvested in cold PBS with protease inhibitor (Roche). Cells were lysed for 20 min on ice in lysis buffer (30 mM Tris, pH7.5, 150 mM NaCl, 1% Triton X-100). The lysates were cleared by

centrifugation at 14,000 rpm for 10 min and then incubated with anti-DR5 mAb 5C7 or anti-C8 (Santa Cruz Biotechnology) conjugated beads overnight at 4°C. IP beads were subsequently washed four times with lysis buffer and boiled in SDS sample buffer for 10 min. Samples were then analyzed by SDS-PAGE followed by immunoblot.

Size-Exclusion Chromatography
Cells were lysed in Tris-buffered saline containing 1% Triton X-100 and protease inhibitor (Roche). Lysates were spun at maximum speed, and supernatants were loaded onto a Superdex 200 10/300 GL column (GE Healthcare). Fractions were collected in 0.5 ml volumes and analyzed by caspase-8 activity assay, or immunoprecipitated with DR5 Ab and immunoblotted for DR5.

Chemical crosslinking
For chemical crosslinking, cells were lysed with PBS buffer containing 1% Triton X-100. Lysates were spun at maximum speed, and 1 mM of DTSSP (Pierce) was added to supernatants for 1 hr at 4°C. Cross-linking was quenched by the addition of Tris, pH7.5, at a final concentration of 30 mM.

Immunofluorescence
For immunostaining, cells cultured on Lab-TekII Chamber slides were washed three times in PBS, fixed for 20 min in 4% paraformaldehyde (EMS) at room temperature, washed, and permeabilized with 0.1% Triton X-100 for 10 min at room temperature. The slides were then treated with 5% goat serum (Jackson ImmunoResearch) in 3% BSA/PBS for 1 hr at room temperature. Abs were diluted in blocking buffer and incubated with cells at 4°C overnight. After three washes with PBS, cells were incubated with secondary antibodies conjugated to Alexa 488 or Alexa 568 (Invitrogen) for 1 hr at room temperature. Slides were mounted with Prolong Gold anti-fade reagent with DAPI and viewed with a Zeiss LSM510 upright confocal microscope or Leica SP5 inverted confocal microscope.

Flow cytometry
Surface expression of DR5 was determined by fluorescence activated cell sorting (FACS). Cells were stained with 2 μg/ml primary anti-DR5 mAb 3H3, or a mouse IgG control Ab (BD BioScience) for 1 hr at 4°C. Cells were then washed with PBS and incubated with a Alexa 488-conjugated secondary antibody (Invitrogen) for 30 min at 4°C. Cells were analyzed by flow cytometry using a FACS Calibur flow cytometer (Becton Dickinson Immunocytometry).

QPCR
TNFRSF10A, TNFRSF10B, TNFSF10, TNFRSF1A, FAS, ERN1, XBP1, DDIT3, PPP1R15A, and *ERO1L* transcript expression levels were assessed by QPCR using standard TaqMan techniques. Transcript levels were normalized to the housekeeping genes *GAPDH* or *RPL19* and results are expressed as normalized expression values ($=2^{-\Delta_{Ct}}$). Primer/probe sets were purchased from Invitrogen.

Generation of RNAs encoding human DR5 isoforms
The coding sequences of human DR5S (isoform 1) and DR5L (isoform 2) were amplified from cDNAs obtained from HEK293T cells using Phusion DNA polymerase (New England Biolabs). An *EcoRI* site and a minimal T7 promoter were engineered into the 5' oligonucleotide and a *BamHI* site was engineered into the 3' oligonucleotide. The oligonucleotide sequences are the following:
hDR5_EcoRI_T7:
5'-CATCATgaattcTAATACGACTCACTATAGGCCATGGAACAACGGGGACA-3';
hDR5_BamHI:
5'-CATCATggatcCTTAGGACATGGCAGAGTCT-3'.

Gel-purified PCR products were then subcloned into the cognate sites of pUC19 (Invitrogen). Positive clones were then digested with *BamHI* and 1 μg of each purified linear plasmid were

used for in vitro transcription reactions using T7 RNA polymerase (New England Biolabs). The reaction products were treated with DNase and run on a 6% TBE-Urea PAGE gel. The products of the expected sizes were excised from the gel and recovered using the crush-and-soak method. The RNA was then precipitated with 300 mM sodium acetate and one volume of isopropanol. The RNA pellets were then washed with cold 80% ethanol and dissolved in 5 μl of RNA resuspension buffer (20 mM HEPES pH 7.5, 100 mM NaCl and 1 mM $Mg(OAc)_2$. The purified RNAs were subsequently radiolabeled and used for in vitro cleavage assays.

Radiolabeling of RNAs encoding human DR5 isoforms

Prior to radiolabeling the RNAs encoding human DR5 isforms, 1.2 μg of the purified transcripts were treated with calf intestine alkaline phosphatase (New Englad Biolabs) to remove the terminal phosphates from the 5' overhangs. The RNAs were then purfied by acid phenol:chloroform extraction and subsequently labeled with T4 polynucleotide kinase (New Englad Biolabs) using 70 μCi ^{32}P-ATP. To remove unincorporated ^{32}P-ATP the RNAs were extracted again with acid phenol:chloroform, precipitated with 300 mM NaOAc and one volume of isopropanol. The RNA pellets were then washed with cold 80% ethanol and dissolved in 5 μl of RNA resuspension buffer (20 mM HEPES pH 7.5, 100 mM NaCl and 1 mM $Mg(OAc)_2$. 20% of the purified, radiolabeled RNAs were subsequently used for in vitro cleavage assays.

Generation of recombinant proteins

Human IRE1α KR43 was expressed and purified in SF21 cells. Cloning into pFast bac HT vector and the sequence of IRE1α KR43 was previously described (*28*). Expression was performed as described in BAC-TO-BAC baculovirus expression system (Life Technologies). SF21 cells were grown in serum-free SF-900 II SFM media at 28°C in plastic disposable Erlenmeyer flasks shaking at 150 rpm. The bacmid DNA was transfected into SF21 cells, and then the virus was amplified two more times at a low MOI before infection of SF21 cells for expression. After 72 hr of expression, the cells were isolated from media using centrifugation. Cells were then lysed in buffer containing 20 mM Tris-HCl, pH 7.5, 600 mM NaCl, 2 mM $MgCl_2$, 3 mM imidazole, 10% glycerol, 1% Triton X-100, 3 mM 2-mercaptoethanol, protease inhibitors (Roche), and PhosSTOP phosphatase inhibitor cock (Roche) and passed 3 times through an Emulsiflex-C3 homogenizer (Avestin) for complete lysis. Lysate was cleared using centrifugation at 100,000 x g. The human IRE1α was N-terminally tagged with a hexa-histidine epitope and was purified using Ni-NTA agarose (Qiagen). Lysate was allowed to incubate on beads for 2 hr before being washed 3 times with buffer containing 20 mM Tris-HCl, pH 7.5, 600 mM NaCl, 2 mM $MgCl_2$, 30 mM imidazole, 10% glycerol and 3 mM 2-mercaptoethanol. Protein was eluted from column by raising the imidazole concentration to 250 mM. Human IRE1α was passed through a HiTrap desalting column (GE Healthcare) before being loaded on a Mono-Q 5/50 GL column (GE Healthcare). For further purification the protein was then concentrated and loaded on to a Superdex 200 HR 10/300 (GE Healthare) column in buffer containing 20 mM Hepes pH 7.5, 250 mM NaCl 1 mM $MgCl_2$, 5% Glycerol, 5 mM DTT, and 5 mM Octyl b-D-glucopyranoside. The protein was then stored at -80°C. *Saccharomyces cerevisiae* Ire1 KR32 was purified as previously described (*29*). Purified recombinant protein was stored in buffer containing 20 mM HEPES pH 7.1, 300 mM NaCl, 2 mM $MgCl_2$, 5% glycerol, and 5 mM DTT, and stored at -80^{o}C.

In vitro cleavage assay

For in vitro cleavage assays, 1 μl (20%) of the 5-^{32}P-labeled RNAs encoding human DR5S and DR5L were incubated with the recombinant kinase/nuclease domains of human IRE1-alpha (KR43) or yeast (*S. cereviseae*) Ire1 (KR32) in cleavage buffer (20 mM HEPES pH 7.5, 70 mM NaCl, 2 mM $Mg(OAc)_2$, 2 mM ADP, 4 mM DTT and 5% glycerol) in a final volume of 10 μl for the indicated times. Stop buffer (10 M urea, 01% SDS, 1 mM EDTA, 0.05% xylene cyanol, 0.05% bromophenol blue) was added and the reactions were heated at 80^{o}C for 3 min prior to loading 2 μl of the cleavage products on each lane of a 5% TBE-Urea PAGE gel, stained with SYBR Gold and photographed in a UV-transilluminator.

Statistical analysis

Where appropriate, we assessed the statistical significance of the difference between two sets of data using an unpaired, two-tailed *t*-test or a paired *t*-test for control and experimental data groups that could be paired. Differences were considered statistically significant (marked with an asterisk) at 5% or less.

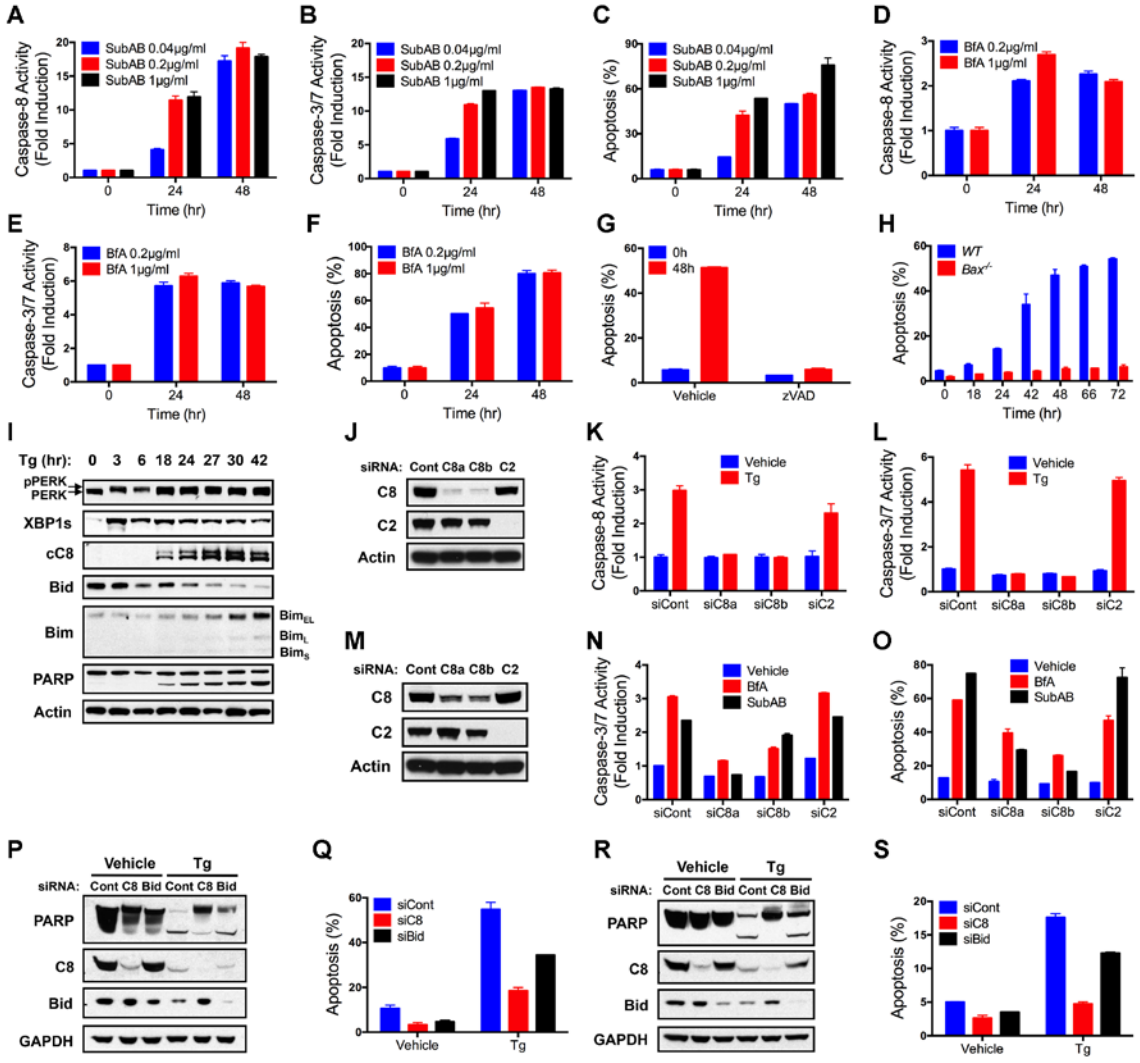

Fig. S1. Unmitigated ER stress triggers apoptosis via caspase-8. (**A** to **C**) KMS11 cells were incubated with SubAB at the indicated dose and time and analyzed by enzymatic assay for caspase-8 (**A**) or caspase-3/7 (**B**) activity or by FACS for apoptosis based on sub-G1 DNA content (**C**). (**D** to **F**) KMS11 cells were incubated with BfA at the indicated dose and time and analyzed by enzymatic assay for caspase-8 (**D**) or caspase-3/7 (**E**) activity or by FACS for apoptosis (**F**). (**G**) HCT116 cells were treated for 48 hr with Tg (100 nM) in absence or presence of the pan caspase inhibitor zVAD-fmk and analyzed by FACS for apoptosis. (**H**) Wildtype (WT) and Bax-knockout (*Bax*$^{-/-}$) HCT116 cells were treated with Tg (100 nM) for the indicated time and analyzed by FACS for apoptosis. (**I**) HCT116 cells were treated with Tg (100 nM) for the indicated time and protein markers were analyzed by immunoblot as noted. (**J** to **L**) HCT116 cells were transfected for 48 hr with a control siRNA (Cont) or a single siRNA targeting caspase-8 (C8a), or an independent pool of siRNAs targeting the same (C8b), or an siRNA targeting caspase-2 (C2). The cells were analyzed by immunoblot for knockdown efficiency (**J**), or treated for 24 hr with Tg (100 nM) and analyzed by enzymatic assay for activity of caspase-8 (**K**) or caspase-3/7 (**L**). (**M** to

O) SK-MES-1 cells were transfected as in (**J**). The cells were analyzed by immunoblot for knockdown efficiency (**M**), or treated for 24 hr with BfA (1 μg/ml) or SubAB (1 μg/ml), and analyzed by enzymatic assay for caspase-3/7 activity (**N**), or by FACS for apoptosis (**O**). (**P** and **Q**) HCT116 were transfected for 48 hr with a control siRNA (Cont), an siRNA targeting caspase-8 (C8), or an siRNA targeting Bid (Bid). Cells were treated with Tg (100 nM) and analyzed by immunoblot (**P**) or by FACS to measure apoptosis (**Q**). (**R** and **S**) SK-MES-1 were transfected and treated as in (**P**). Cells were analyzed by immunoblot (**R**) or by FACS to measure apoptosis (**S**). Graphed data depict means ± SD of triplicates (for caspase activity) or duplicates (for apoptosis).

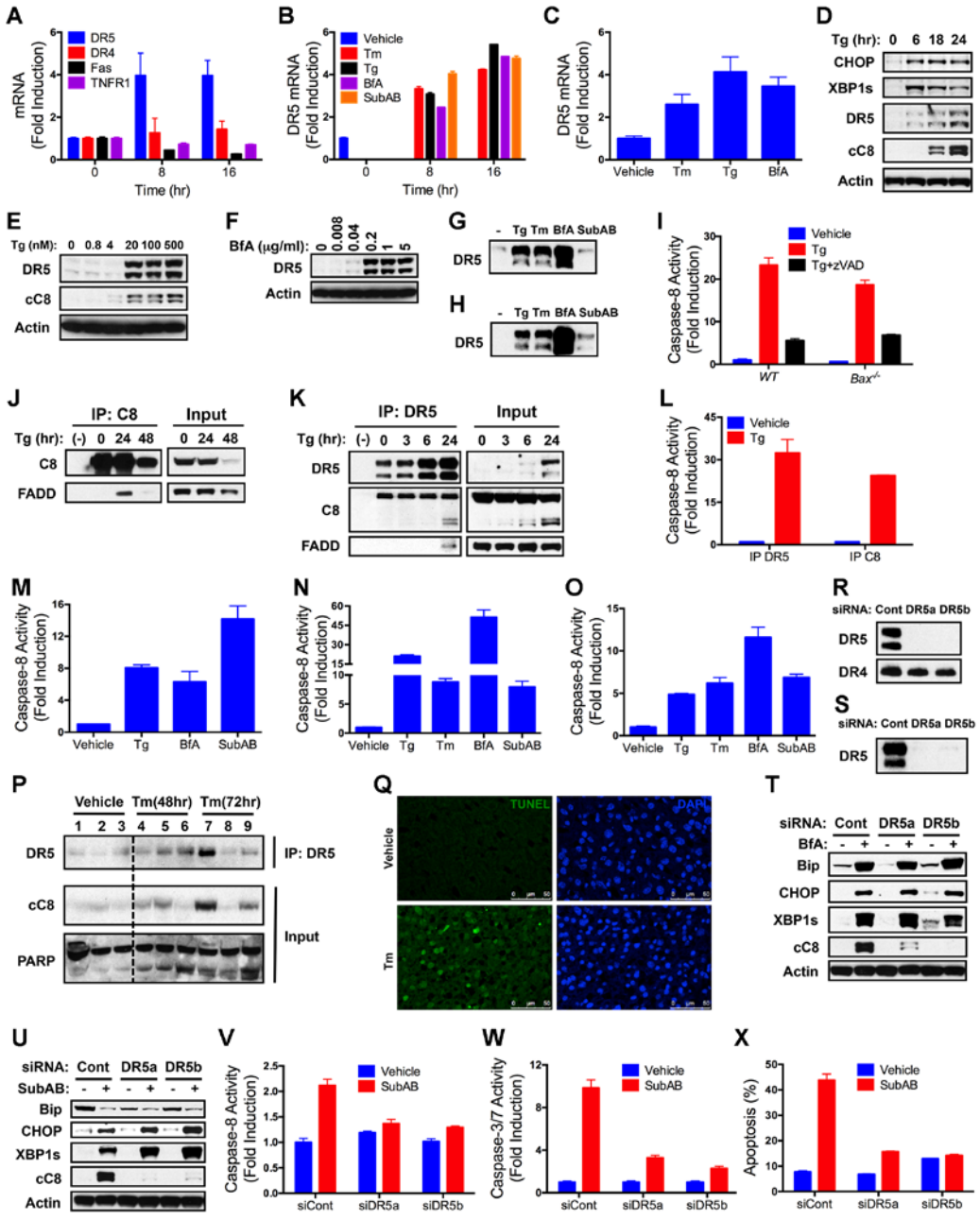

Fig. S2. Unmitigated ER stress activates caspase-8 via DR5. (A) SK-MES-1 cells were treated with Tg (100 nM) for the indicated time, and mRNA levels of the noted death receptors were analyzed by QPCR. The data are normalized to *RPL19* mRNA levels. (**B**) SK-MES-1 cells were

treated for the indicated time with Tm (1 μg/ml), Tg (100 nM), BfA (1 μg/ml), or SubAB (1 μg/ml). *DR5* mRNA levels were analyzed by QPCR. The data are normalized to *GAPDH* mRNA levels. (**C**) RPMI8226 cells were treated for 8 hr with Tm, Tg, or BfA (same doses as in **B**) and *DR5* mRNA levels were determined as in (**B**). (**D**) SK-MES-1 cells were treated with Tg (100 nM) for the indicated time and the noted protein markers were analyzed by immunoblot. (**E**) HCT116 cells were treated for 24 hr with Tg at the indicated dose and the noted markers were analyzed by immunoblot. (**F**) SK-MES-1 cells were treated for 24 hr with BfA at the indicated dose and the noted markers were analyzed by immunoblot. (**G** and **H**) RPMI8226 (**G**) or KMS11 (**H**) cells were treated for 24 hr with Tg, Tm, BfA, or SubAB (same doses as in **B**) and DR5 was analyzed by immunoblot. (**I**) HCT116 cells were treated for 24 hr with Tg (100 nM) in the absence or presence of zVAD (20 μM), subjected to DR5 IP, and caspase-8 activity in IPs was measured by enzymatic assay. (**J**) HCT116 cells were treated for 24 hr with Tg (100 nM), subjected to caspase-8 IP and analyzed by immunoblot. (**K**) KMS11 cells were treated for 24 hr with Tg (100 nM), subjected to DR5 IP and analyzed by immunoblot. (**L**) HCT116 cells were treated for 24 hr with Tg (100 nM), subjected to DR5 IP or caspase-8 IP and analyzed for caspase-8 activity by enzymatic assay. (**M** to **O**) SK-MES-1 (**M**), KMS11 (**N**), or RPMI8226 (**O**) cells were treated for 24 hr with Tg, Tm, BfA, or SubAB as noted (same doses as in **B**), subjected to DR5 IP, and caspase-8 activity in IPs was determined by enzymatic assay. (**P** and **Q**) Mice were injected i.p. with Tm (1 mg/kg) or carrier (150 mM dextrose). Livers were collected and analyzed by immunoblot at indicated times (**P**) or by immunofluorescence for TUNEL staining indicating apoptosis at 48 hr (**Q**). (**R** and **S**) HCT116 (**R**) or SK-MES-1 (**S**) cells were transfected for 48 hr with control siRNA (Cont) or a single siRNA targeting DR5 (DR5a), or an independent pool of siRNAs targeting the same (DR5b): The cells were analyzed for knockdown efficiency by immunoblot. (**T** to **X**) SK-MES-1 cells were transfected as in (**S**), treated with BfA (1 μg/ml) (**T**) or SubAB (1 μg/ml) (**U** to **X**) for 48 hr, and analyzed by immunoblot (**T** and **U**), or by enzymatic assay for caspase-8 (**V**) or caspase-3/7 (**W**) activity, or by FACS for apoptosis (**X**). Graphed data depict means ± SD of triplicates (for RT-PCR and caspase activity) or duplicates (for caspase activity after IP and apoptosis).

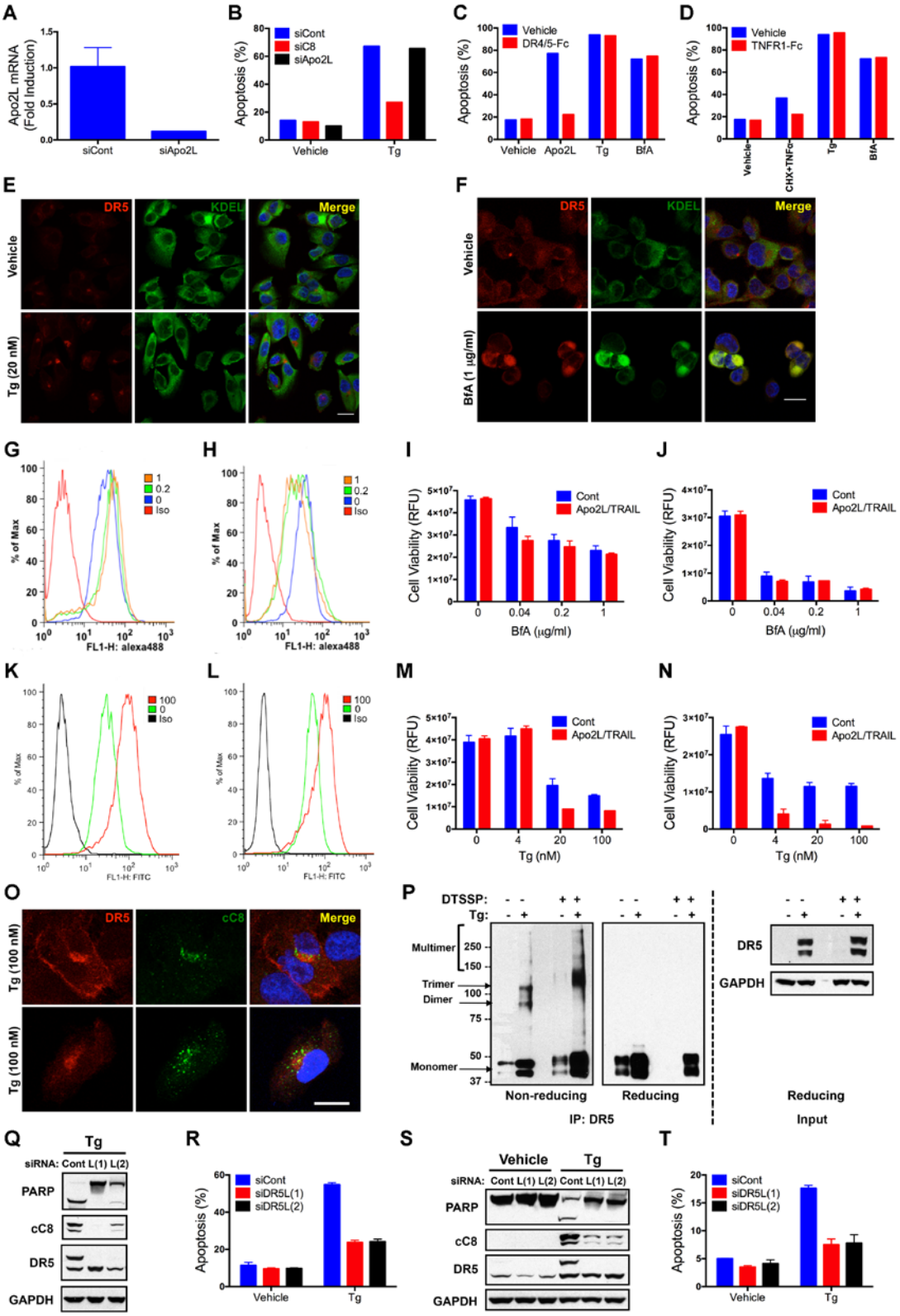

Fig. S3 Unmitigated ER stress induces ligand-independent intracellular DR5 activation to engage caspase-8. (**A**) HCT116 cells were transfected for 48 hr with control siRNA or siRNA targeting Apo2L/TRAIL and knockdown efficiency was analyzed by QPCR. Values are normalized

to *GAPDH* mRNA. (**B**) SK-MES-1 cells were transfected for 48 hr with control siRNA or siRNA targeting caspase-8 or Apo2L/TRAIL, treated for 24 hr with Tg (100 nM), and analyzed by FACS for apoptosis. (**C** and **D**) HCT116 cells were treated for 48 hr with Apo2L/TRAIL (1 μg/ml) or Tg (100 nM) or BfA (1 μg/ml) in the absence or presence of DR4-Fc plus DR5-Fc (10 μg/ml each) (**C**), or with TNFα (100 ng/ml) plus cycloheximide (CHX; 1 μM) in the absence or presence of TNFR1-Fc (10 μg/ml) (**D**) and analyzed by FACS for apoptosis. (**E** and **F**) SK-MES-1 cells were treated for 24 hr with Tg (20 nM) (**E**) or BfA (1 μg/ml) (**F**) and analyzed by immunofluorescence with a specific antibody to DR5, the ER marker KDEL, or both (Merge). (**G** and **H**) HCT116 (**G**) or SK-MES-1 (**H**) cells were treated for 24 hr with indicated BfA concentrations (μg/ml) and cell-surface levels of DR5 were determined by FACS with DR5-specific antibody or control IgG. (**I** and **J**) HCT116 (**I**) or SK-MES-1 (**J**) cells were treated for 24 hr with indicated BfA concentration followed by Apo2L/TRAIL (4 ng/ml) for an additional 24 hr, and analyzed for viability by Cell Titer Glo assay. (**K** and **L**) HCT116 (**K**) or SK-MES-1 (**L**) cells were treated for 24 hr with the indicated Tg concentration (nM) and cell-surface levels of DR5 were determined by FACS. (**M** and **N**) HCT116 (**M**) or SK-MES-1 (**N**) cells were treated for 24 hr with the indicated Tg concentration followed by Apo2L/TRAIL (4 ng/ml) for an additional 24 hr ,and analyzed for cell viability. (**O**) SK-MES-1 cells were treated for 24 hr with Tg (20 nM) and zVAD (20 μM) and analyzed by immunofluorescence with specific antibody to DR5, cleaved caspase-8 (cC8), or both (Merge). Two examples of Tg-treated cells are shown. (**P**) HCT116 cells were treated with Tg (100 nM) for 24 hr. Cells were lysed and subjected to chemical crosslinking with DTSSP (1 mM), followed by DR5 IP and analysis by immunoblot under non-reducing or reducing conditions as noted. (**Q** and **R**) HCT116 were transfected for 48 hr with a control siRNA (Cont), or two independent siRNAs against DR5L [L(1) or L(2)]. Cells were treated with Tg (100 nM) and analyzed by immunoblot (**Q**) or by FACS to measure apoptosis (**R**). (**S** and **T**) SK-MES-1 were transfected and treated as in (**Q**). Cells were analyzed by immunoblot (**S**) or FACS (**T**). Graphed data depict means ± SD of triplicates. Scale bar: 20 μM

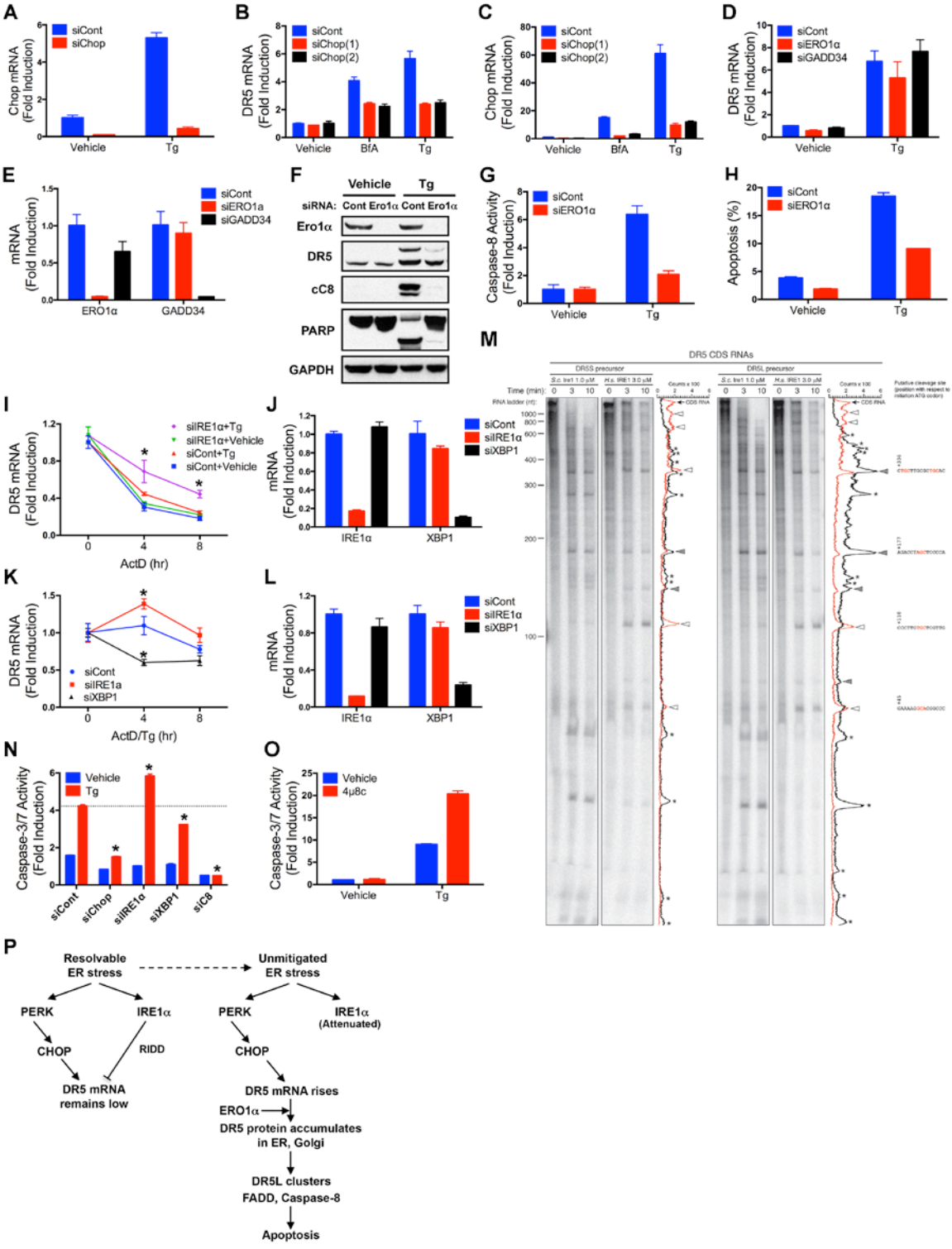

Fig. S4 DR5 integrates opposing signals from CHOP and IRE1α to control apoptosis activation. (**A**) HCT116 cells were transfected for 48 hr with control siRNA or siRNA targeting CHOP, and knockdown efficiency was analyzed by Q-RT-PCR. Values are normalized to *GAPDH* mRNA. (**B** and **C**) SK-MES-1 cells were transfected for 48 hr with control siRNA or independent siRNAs targeting CHOP. The cells were treated with BfA (1 μg/ml) for 8 hr or Tg (100 nM) for 16

hr and analyzed as in (**A**) for levels of *DR5* mRNA (**B**) or *CHOP* mRNA (**C**). (**D** and **E**) HCT116 cells were transfected for 48 hr with control siRNA, an siRNA targeting ERO1α, or an siRNA targeting GADD34. The cells were treated with Tg (100 nM) for 16 hr and analyzed as in (**A**) for levels of *DR5* mRNA (**D**) or *ERO1α* or *GADD34* mRNA (**E**). (**F** to **H**) HCT116 cells were transfected for 48 hr with control siRNA or an siRNA targeting ERO1α, treated with Tg (100 nM) for 24 hr, and analyzed by immunoblot (**F**), or by enzymatic assay for caspase-8 activity (**G**), or by FACS for apoptosis (**H**). (**I**) HCT116 cells were transfected (48 hr) with control or IRE1α siRNA, treated with vehicle or Tg (20 nM) in presence of actinomycin D (2 μg̃ml) to block de novo transcription, and *DR5* mRNA was measured by Q-RT-PCR (normalized to *RPL19* mRNA). (**J**) HCT116 cells were transfected for 48 hr with control, IRE1α, or XBP1 siRNA and knockdown efficiency was analyzed as in (**A**). (**K**) SK-MES-1 cells were transfected for 48 hr with control, IRE1α, or XBP1 siRNA. Cells were treated for the indicated time with Tg (20 nM) in presence of actinomycin D (2 μg/ml). DR5 mRNA levels were then determined. (**L**) SK-MES-1 cells were transfected for 48 hr with control, IRE1α, or XBP1 siRNA and knockdown efficiency was analyzed. (**M**) 5'-^{32}P-labeled transcripts encoding human *DR5* mRNA splice isoforms were incubated with recombinant human IRE1α KR43 or yeast (*Saccharomyces cerevisiae*) Ire1 KR32 for the indicated times. The reactions were run on a 5% TBE-Urea PAGE gel and exposed for one week to a blank phosphorscreen. The screen was then scanned with a Typhoon Variable-Mode Imager (GE Life Sciences) using a 50 μm pixel size resolution. Traces on the right panels show quantification of the scans. Red traces correspond to quantification of cleavage products by human IRE1α at 10 min. Black traces correspond to quantification of cleavage products by yeast Ire1 at 10 min. White arrowheads indicate cleavage products that are specifically generated by human IRE1α. Asterisks indicate cleavage products specifically generated by yeast Ire1. The position with respect to the initiation codon and sequence of the most prominent putative cleavage sites, as previously defined (*30*), are indicated on the right. (**N**) HCT116 cells were transfected for 48 hr with the indicated siRNA, treated with vehicle or Tg (100 nM) for 24 hr, and analyzed for caspase-3/7 activity. (**O**) HCT116 cells were treated for 24 hr with vehicle or Tg (100 nM) in presence of vehicle or the IRE1α endonuclease inhibitor 4μ8c (30 μM), and analyzed for caspase-3/7 activity. (**P**) Model for UPR-controlled, intracellular DR5-mediated apoptosis activation. See text for detailed description. Graphed data depict means ± SD of triplicates.

References

1. P. Walter, D. Ron, The unfolded protein response: From stress pathway to homeostatic regulation. *Science* **334**, 1081–1086 (2011). Medline doi:10.1126/science.1209038

2. C. Hetz, The unfolded protein response: Controlling cell fate decisions under ER stress and beyond. *Nat. Rev. Mol. Cell Biol.* **13**, 89–102 (2012). Medline

3. A. Korennykh, P. Walter, Structural basis of the unfolded protein response. *Annu. Rev. Cell Dev. Biol.* **28**, 251–277 (2012). Medline doi:10.1146/annurev-cellbio-101011-155826

4. J. Hollien, J. S. Weissman, Decay of endoplasmic reticulum-localized mRNAs during the unfolded protein response. *Science* **313**, 104–107 (2006). Medline doi:10.1126/science.1129631

5. S. Wang, R. J. Kaufman, The impact of the unfolded protein response on human disease. *J. Cell Biol.* **197**, 857–867 (2012). Medline doi:10.1083/jcb.201110131

6. I. Tabas, D. Ron, Integrating the mechanisms of apoptosis induced by endoplasmic reticulum stress. *Nat. Cell Biol.* **13**, 184–190 (2011). Medline doi:10.1038/ncb0311-184

7. N. N. Danial, S. J. Korsmeyer, Cell death: Critical control points. *Cell* **116**, 205–219 (2004). Medline doi:10.1016/S0092-8674(04)00046-7

8. G. S. Salvesen, A. Ashkenazi, Snapshot: Caspases. *Cell* **147**, 476, e1 (2011). Medline doi:10.1016/j.cell.2011.09.030

9. H. Zinszner, M. Kuroda, X. Wang, N. Batchvarova, R. T. Lightfoot, H. Remotti, J. L. Stevens, D. Ron, CHOP is implicated in programmed cell death in response to impaired function of the endoplasmic reticulum. *Genes Dev.* **12**, 982–995 (1998). Medline doi:10.1101/gad.12.7.982

10. H. Puthalakath, L. A. O'Reilly, P. Gunn, L. Lee, P. N. Kelly, N. D. Huntington, P. D. Hughes, E. M. Michalak, J. McKimm-Breschkin, N. Motoyama, T. Gotoh, S. Akira, P. Bouillet, A. Strasser, ER stress triggers apoptosis by activating BH3-only protein Bim. *Cell* **129**, 1337–1349 (2007). Medline doi:10.1016/j.cell.2007.04.027

11. J.-P. Upton, L. Wang, D. Han, E. S. Wang, N. E. Huskey, L. Lim, M. Truitt, M. T. McManus, D. Ruggero, A. Goga, F. R. Papa, S. A. Oakes, IRE1α cleaves select microRNAs during ER stress to derepress translation of proapoptotic Caspase-2. *Science* **338**, 818–822 (2012). Medline doi:10.1126/science.1226191

12. J. J. Sandow, L. Dorstyn, L. A. O'Reilly, M. Tailler, S. Kumar, A. Strasser, P. G. Ekert, ER stress does not cause upregulation and activation of caspase-2 to initiate apoptosis. *Cell Death Differ.* **21**, 475–480 (2014). Medline doi:10.1038/cdd.2013.168

13. A. W. Paton, T. Beddoe, C. M. Thorpe, J. C. Whisstock, M. C. Wilce, J. Rossjohn, U. M. Talbot, J. C. Paton, AB5 subtilase cytotoxin inactivates the endoplasmic

reticulum chaperone BiP. *Nature* **443**, 548–552 (2006). Medline doi:10.1038/nature05124

14. J. H. Lin, H. Li, D. Yasumura, H. R. Cohen, C. Zhang, B. Panning, K. M. Shokat, M. M. Lavail, P. Walter, IRE1 signaling affects cell fate during the unfolded protein response. *Science* **318**, 944–949 (2007). Medline doi:10.1126/science.1146361

15. H. Li, H. Zhu, C. J. Xu, J. Yuan, Cleavage of BID by caspase 8 mediates the mitochondrial damage in the Fas pathway of apoptosis. *Cell* **94**, 491–501 (1998). Medline doi:10.1016/S0092-8674(00)81590-1

16. H. LeBlanc, D. Lawrence, E. Varfolomeev, K. Totpal, J. Morlan, P. Schow, S. Fong, R. Schwall, D. Sinicropi, A. Ashkenazi, Tumor-cell resistance to death receptor–induced apoptosis through mutational inactivation of the proapoptotic Bcl-2 homolog Bax. *Nat. Med.* **8**, 274–281 (2002). Medline doi:10.1038/nm0302-274

17. N. S. Wilson, V. Dixit, A. Ashkenazi, Death receptor signal transducers: Nodes of coordination in immune signaling networks. *Nat. Immunol.* **10**, 348–355 (2009). Medline doi:10.1038/ni.1714

18. H. Yamaguchi, H. G. Wang, CHOP is involved in endoplasmic reticulum stress-induced apoptosis by enhancing DR5 expression in human carcinoma cells. *J. Biol. Chem.* **279**, 45495–45502 (2004). Medline doi:10.1074/jbc.M406933200

19. J. P. Sheridan, S. A. Marsters, R. M. Pitti, A. Gurney, M. Skubatch, D. Baldwin, L. Ramakrishnan, C. L. Gray, K. Baker, W. I. Wood, A. D. Goddard, P. Godowski, A. Ashkenazi, Control of TRAIL-induced apoptosis by a family of signaling and decoy receptors. *Science* **277**, 818–821 (1997). Medline doi:10.1126/science.277.5327.818

20. M. Abdelrahim, K. Newman, K. Vanderlaag, I. Samudio, S. Safe, 3,3′-Diindolylmethane (DIM) and its derivatives induce apoptosis in pancreatic cancer cells through endoplasmic reticulum stress-dependent upregulation of DR5. *Carcinogenesis* **27**, 717–728 (2006). Medline doi:10.1093/carcin/bgi270

21. B. C. S. Cross, P. J. Bond, P. G. Sadowski, B. K. Jha, J. Zak, J. M. Goodman, R. H. Silverman, T. A. Neubert, I. R. Baxendale, D. Ron, H. P. Harding, The molecular basis for selective inhibition of unconventional mRNA splicing by an IRE1-binding small molecule. *Proc. Natl. Acad. Sci. U.S.A.* **109**,E869–E878 (2012). Medline doi:10.1073/pnas.1115623109

22. L. Niederreiter, T. M. Fritz, T. E. Adolph, A. M. Krismer, F. A. Offner, M. Tschurtschenthaler, M. B. Flak, S. Hosomi, M. F. Tomczak, N. C. Kaneider, E. Sarcevic, S. L. Kempster, T. Raine, D. Esser, P. Rosenstiel, K. Kohno, T. Iwawaki, H. Tilg, R. S. Blumberg, A. Kaser, ER stress transcription factor Xbp1 suppresses intestinal tumorigenesis and directs intestinal stem cells. *J. Exp. Med.* **210**, 2041–2056 (2013). Medline doi:10.1084/jem.20122341

23. K. W. Wagner, E. A. Punnoose, T. Januario, D. A. Lawrence, R. M. Pitti, K. Lancaster, D. Lee, M. von Goetz, S. F. Yee, K. Totpal, L. Huw, V. Katta, G. Cavet, S. G. Hymowitz, L. Amler, A. Ashkenazi, Death-receptor O-glycosylation

controls tumor-cell sensitivity to the proapoptotic ligand Apo2L/TRAIL. *Nat. Med.* **13**, 1070–1077 (2007). Medline doi:10.1038/nm1627

24. R. Martín-Pérez, M. Niwa, A. López-Rivas, ER stress sensitizes cells to TRAIL through down-regulation of FLIP and Mcl-1 and PERK-dependent up-regulation of TRAIL-R2. *Apoptosis* **17**, 349–363 (2012). Medline doi:10.1007/s10495-011-0673-2

25. P. Hu, Z. Han, A. D. Couvillon, R. J. Kaufman, J. H. Exton, Autocrine tumor necrosis factor alpha links endoplasmic reticulum stress to the membrane death receptor pathway through IRE1alpha-mediated NF-kappaB activation and down-regulation of TRAF2 expression. *Mol. Cell. Biol.* **26**, 3071–3084 (2006). Medline doi:10.1128/MCB.26.8.3071-3084.2006

26. L. Zhang, J. Yu, B. H. Park, K. W. Kinzler, B. Vogelstein, Role of BAX in the apoptotic response to anticancer agents. *Science* **290**, 989–992 (2000). Medline doi:10.1126/science.290.5493.989

27. S. M. Chamow, A. Ashkenazi, Immunoadhesins: Principles and applications. *Trends Biotechnol.* **14**, 52–60 (1996). Medline doi:10.1016/0167-7799(96)80921-8

28. H. Li, A. V. Korennykh, S. L. Behrman, P. Walter, Mammalian endoplasmic reticulum stress sensor IRE1 signals by dynamic clustering. *Proc. Natl. Acad. Sci. U.S.A.* **107**, 16113–16118 (2010). Medline doi:10.1073/pnas.1010580107

29. A. V. Korennykh, P. F. Egea, A. A. Korostelev, J. Finer-Moore, C. Zhang, K. M. Shokat, R. M. Stroud, P. Walter, The unfolded protein response signals through high-order assembly of Ire1. *Nature* **457**, 687–693 (2009). Medline doi:10.1038/nature07661

30. P. Kimmig, M. Diaz, J. Zheng, C. C. Williams, A. Lang, T. Aragón, H. Li, P. Walter, The unfolded protein response in fission yeast modulates stability of select mRNAs to maintain protein homeostasis. *Elife* **1**, e00048 (2012). Medline doi:10.7554/eLife.00048